Conf-940424--32

# BUGLE-93 (ENDF/B-VI) CROSS-SECTION LIBRARY DATA TESTING USING SHIELDING BENCHMARKS

Hamilton T. Hunter**
Charles O. Slater
J. E. White
Oak Ridge National Laboratory
Oak Ridge, Tennessee 37831-6363



to be presented at the
American Nuclear Society
Topical Meeting
8th International Conference on
Radiation Shielding
April 24 - 28, 1994
Arlington, Texas



*Research sponsored by the U.S. Department of Energy.
**Managed by Martin Marietta Energy Systems, Inc. for the U. S. Department of Energy under Contract DE-AC05-84OR21400.

# BUGLE-93 (ENDF/B-VI) CROSS-SECTION LIBRARY DATA TESTING USING SHIELDING BENCHMARKS

H. T. Hunter, C. O. Slater*, and J. E. White
Oak Ridge National Laboratory
P.O. Box 2008
Oak Ridge, Tennessee 37831-6362
(615) 574-6176 *(615) 574-6105

## ABSTRACT

Several integral shielding benchmarks were selected to perform data testing for new multigroup cross-section libraries compiled from the ENDF/B-VI data for light water reactor (LWR) shielding and dosimetry. The new multigroup libraries, BUGLE-93 and VITAMIN-B6, were studied to establish their reliability and response to the benchmark measurements by use of radiation transport codes, ANISN and DORT. Also, direct comparisons of BUGLE-93 and VITAMIN-B6 to BUGLE-80 (ENDF/B-IV) and VITAMIN-E (ENDF/B-V) were performed. Some benchmarks involved the nuclides used in LWR shielding and dosimetry applications, and some were sensitive to specific nuclear data, i.e. iron due to its dominant use in nuclear reactor systems and complex set of cross-section resonances. Five shielding benchmarks (four experimental and one calculational) are described and results are presented.

## I. INTRODUCTION

About ten years ago, the ANSI/ANS 6.1.2 standard was issued describing the methodology for producing multigroup cross sections for nuclear power plant shielding analyses. This methodology has been used to update the older multigroup libraries, BUGLE-80[1] (ENDF/B-IV) and VITAMIN-E[2] (ENDF/B-V) with the more accurate ENDF/B-VI data. These new libraries are BUGLE-93[3] and VITAMIN-B6[3]. The fine-group (199 neutron/42 gamma) library, VITAMIN-B6, uses an energy group structure based on the European's VITAMIN-J[4] (175 neutron/42 gamma) and SCALE[5] shielding libraries (27 neutron/18 gamma). Further collapse of the new VITAMIN-B6 library into the BUGLE-80 (47 neutron/20 gamma) group structure
was done using the same methodology for producing BUGLE-80 and SAILOR[6]. The new broad-group library, called BUGLE-93, contains 5 separate sets of cross sections, each using a different weighting spectrum based on the flux in a (a) PWR concrete shield, (b) BWR fuel cell, (c) PWR fuel cell, (d) steel-water mixture, and (e) PWR pressure vessel. The flux spectra used to collapse the above five sets of BUGLE-93 data are derived from one-dimensional computations using XSDRNPM[5] with the VITAMIN-B6 library.

## II. DATA TESTING GOALS

The procedures used in producing and testing the new cross-section libraries provided quality assurance by ensuring the reliablity of the new libraries in several different benchmark calculations. The benchmarks have been selected to test both the fine-group and/or broad-group performance in different areas of the nuclear system. Criticality benchmarks were selected to test the reliability of the fine-group cross-section library (VITAMIN-B6) within the reactor core and to test the self-shielding, neutron/gamma-ray production, and the photon interaction cross-section interfaces for proper implementation. The shielding benchmarks tested the new libraries' performance by comparisons to older cross-section libraries.

## III. SHIELDING BENCHMARKS

The VITAMIN-B6 and BUGLE-93 cross sections were tested using integral benchmarks selected from the Cross Section Evaluation Working Group (CSEWG), Nuclear Energy Agency Nuclear Science Committee (NEANSC), and other relevant integral shielding benchmarks. The cross-section libraries, BUGLE-80 and VITAMIN-E, were used in the calculations to give direct comparisons of BUGLE-93 and VITAMIN-B6 results for each benchmark.

The shielding benchmarks are listed below.

CSEWG:

- *1) SDT11: ORNL Benchmark for Iron and Stainless Steel.
- 2) SB2: Secondary Gamma-Ray Production for Thermal Neutron Spectrum.
- 3) SB3: Secondary Gamma-Ray Production for Fast Neutron Spectrum.
- 4) SDT1-4: "Broomstick" Experiments for Iron, Oxygen, Nitrogen, and Sodium.

NEANSC:

- *1) Winfrith Iron Benchmark Experiment.
- 2) Winfrith Water Benchmark Experiment.
- 3) PWR Computational Shielding Benchmark.
- 4) LMFBR Computational Shielding Benchmark.

Other Relevant Benchmarks:

- *1) University of Illinois Iron Sphere Benchmark.
- *2) PCA-PV "Blind Test" Benchmark.
- 3) Winfrith NESDIP2 and NESDIP3 Radial Shield and Cavity Experiments.
- *4) LWR Computational Shielding Benchmark.

*presented below.

## IV. CALCULATIONS

All calculations for the benchmarks used either ANISN[7] (one-dimensional) or DORT[8] (two-dimensional) discrete ordinates radiation transport codes. The calculations used the BUGLE-93 library which was derived from VITAMIN-B6 and a calculated flux spectrum from the concrete shield region of a one-dimensional light water reactor. This allowed direct comparisons to BUGLE-80. The standard weighted VITAMIN-E and VITAMIN-B6 libraries were used for similar fine-group comparisons. In a few benchmarks, special calculations were done with self-shielded cross sections and zone-specific cross sections. Results from the calculations are plotted together for a visual comparison and tabulated using the ratio of calculated values to experimental values.

## V. DATA TESTING RESULTS

### A. The University of Illinois Iron Sphere Benchmark

This benchmark[9] makes use of either an encapsulated californium (Cf-252) fission source or a deuterium-tritium (D-T) fusion neutron source at the center of a hollow iron sphere with a 7.65 cm inner radius and a 38.1 cm outer radius. The iron sphere is composed of 0.21 wt% carbon 0.47 wt% manganese, 0.013 wt% phosphorous, 0.0024 wt% sulfur, and 99.3046 wt% iron. The fast neutron spectrum, measured using a NE-213 proton recoil spectrometer at 200 cm from the center of the sphere, was reported as neutron leakage per source neutron. The experimental results and those of the ANISN calculations can be seen plotted in Figures 1-6. The BUGLE-93 results show an increase over BUGLE-80 in calculated flux for the energy region above 1 MeV, which more closely matches the experimental results in both the Cf-252 (fission) and D-T (fusion) neutron sources (see Figures 2 and 5). There is a slight improvement using the VITAMIN-B6 library over VITAMIN-E for energies above 3 MeV for both experiments (see Figures 3 and 6).

### B. The SDT11: ORNL Benchmark for Iron and Stainless Steel

The SDT11 experiment[10] was performed at the Tower Shielding Facility, using a collimated neutron beam from the TSR-II reactor (see Figure 7). Various thicknesses of iron or stainless steel were placed at the beam exit. The 30-cm-thick iron and stainless steel calculations are presented here. Measurements of neutron flux behind these shields were completed using a NE-213 liquid scintillator, hydrogen filled Benjamin counters, and 3, 6, and 10 inch Bonner balls, located on and off the reactor centerline. DORT was used with a cylindrical geometry for the calculations. GRTUNCL[11] was used to create a first collision source as input to DORT. The DORT output flux file was then used as input to FALSTF[12]. These codes were necessary for better flux resolution due to possible ray effects. The NE-213 results for 30 cm of iron are presented in Figures 8-10 with resolution smoothed calculations. The count rates for the Bonner balls, the integrated flux from the Benjamin counters, and the off-centerline NE-213 measurements appear with the calculations in Tables 1, 2, and 3, respectively.

The off-centerline measurements eliminate the uncollided portion of flux emanating from the exit of the collimated beam of neutrons. The agreement of the BUGLE-93 and VITAMIN-B6 fast-neutron flux calculations with the off-centerline experimental measurements are within 10-20% but centerline agreement drops to 50-80% agreement. The centerline calculation error is mostly due to the underestimate of uncollided flux coming from deep resonances in iron and is less prevalent in stainless steel. Taking into account this underestimation of the uncollided flux and using the uncollided flux derived from a similar experiment (SDT1[13]), then agreement improves to within 10% (see Figure 10).

### C. The Winfrith Iron Benchmark Experiment

The Winfrith Experiment[14] measured fission neutron transmission through a thick iron shield. The shield consisted of twenty-four 5.08-cm-thick iron plates spaced 6.35 mm apart. Fission neutrons were produced in a natural uranium converter plate which preceded the shield and powered by graphite-moderated neutrons from the NESTOR reactor. The plate's total neutron source per NESTOR Watt is $5.56 \times 10^7$ $s^{-1}$. Neutron spectra were measured at four locations using NE-213 detectors placed in 5.08-cm-wide by 105.5-cm-deep slots cut in special iron plates. In addition, activation foil measurements were made in the gaps between the iron plates.

Calculations for the experiment were performed with DORT using the calculational geometry model and material compositions supplied and fine- and broad-group cross sections from four libraries. Additional calculations were performed using the self-shielded, fine-group cross sections and broad-group cross sections collapsed from the self-shielded fine-group. These were weighted using spectra in several zones within the iron shield. Calculated and measured neutron spectra at 76.2 cm into the shield are presented in Figure 11 for the fine-group calculations and Figure 12 for the broad-group calculations. The calculated results obtained using the self-shielded, VITAMIN-B6 fine-group and the zone-weighted, BUGLE-93 broad-group cross sections are in better agreement with the measured spectrum than are those obtained using the other libraries. Integrals of the calculated neutron spectra at four locations are compared with integrals of the measured spectra in Table 4. For the location at 20.32 cm into the shield, the broad-group libraries and the self-shielded, VITAMIN-B6 library gave calculated integral fluxes about 30% higher than measured, while the standard-weighted, fine-group libraries (VITAMIN-E and VITAMIN-B6) overpredicted about 10%. All libraries underpredict the measured result at 50.8 cm into the shield, and with increasing depth into the shield comes greater underprediction. At 101.6 cm into the shield, the concrete-weighted BUGLE-93 library underpredicted the measured integral flux by greater than a factor of 6. Underpredictions by the other libraries ranged from factors of 1.6 to 4.8. Self-shielding the VITAMIN-B6 cross sections and zone weighting them to produce a BUGLE-93 library led to about a factor of 3.0 increase in the VITAMIN-B6 flux integral and a factor of 3.6 increase in the BUGLE-93 flux integral. Theoretically, the BUGLE-93 flux should approach the VITAMIN-B6 flux as the number of weighting zones in the shield is increased.

Calculated and measured activations are compared in Tables 5 - 7. The high-energy $^{32}S(n,p)$ reaction is affected less by self-shielding than are the $^{103}Rh(n,n')$ and $^{115}In(n,n')$ reactions. For the latter two reactions, whose response functions span the iron resonance regions, self-shielding has a large effect on results at deep penetrations. The calculated $^{115}In(n,n')$ activation shows a greater underprediction than do the $^{103}Rh(n,n')$ results.

D. PCA Blind Test Benchmark

The Pool Critical Assembly (PCA) Blind Test Benchmark[15] was designed to provide measured data against which the shielding methods and data of installations from various countries could be tested. The benchmark was so named because participants were given only the geometry and source description, and calculations were performed without knowledge of the measured data. The geometry represents the radial regions of a typical light water reactor. Several configurations were studied, each being named according to the width (centimeters) of the water layers preceding and following the thermal shield (e.g. for the 12/13 configuration, approximately 12 and 13 cm of water respectively precede and follow the thermal shield). Extensive neutron measurements were made for the 8/7 and 12/13 configurations, and gamma-ray measurements were made for the 4/12 configuration.

While the PCA geometry was parallelepipedal, calculations were performed using DORT with a cylindrical geometry model. For the PCA 4/12 configuration, the gamma-ray spectrum at one location and gamma-ray heating at several locations were calculated. Figure 13 shows a comparison of the calculated and measured gamma-ray spectra for gamma-ray energies between 0.248 and 2.731 MeV. Ratios of the calculated-to-measured flux integrals range from 0.52 to 0.55, so the results from all libraries are essentially comparable. Self-shielding and zone weighting could possibly improve those ratios. Table 8 compares calculated and measured gamma-ray heating results. The calculated gamma-ray heating was obtained by using gamma-ray sensitivities for a $CaF_2$ thermoluminescent dosimeter (TLD). The reported measured results were corrected for neutron contributions to the TLD response. In general, the calculated results agree well with the measured results, the broad-group libraries showing somewhat better agreement. Ratios of gamma-ray heating to the fast-neutron flux at the same locations were also in good agreement with measured values (C/E from 0.84 to 1.12). Therefore, it is puzzling that the calculated integrals of the gamma-ray flux would underpredict the measured integrals to such a degree.

E. The LWR #1 Shielding Benchmark

The LWR Benchmark[16] is a one-dimensional computational benchmark involving 27 elements and 11

zones in a light water reactor model (see Figure 14 and Table 9). The ANISN code results for the gamma and neutron spectra at the concrete outer edge appear in Figures 15 and 16, respectively. No previous reference calculations are available. The BUGLE-93 and VITAMIN-B6 results indicate a small decrease in gamma flux compared to BUGLE-80 and VITAMIN-E at energies below 0.1 MeV and a slight increase above 10 MeV. But overall, the results indicate the libraries are consistent.

## VI. CONCLUSIONS

The BUGLE-93 and VITAMIN-B6 libraries have been tested using several shielding benchmarks. Results were reported for five of those benchmarks and all show that the new libraries are consistent with previous libraries and in some cases better. Improvements to the iron data above 3.0 MeV gave the new libraries a slight edge over the ENDF/B-IV and ENDF/B-V derived libraries in predicting the fast-neutron transmission through thick iron regions. In general, the results showed that for shields containing thick iron regions, problem-specific self-shielded libraries should be used for accurate predictions of neutron transmission through the shield. This was evident for the SDT11 experiment where the greater fraction of the high-energy flux transmitted was due to uncollided neutrons and was underpredicted using total cross sections from the concrete weighted and standard libraries.

## VII. ACKNOWLEDGMENTS

The authors would like to thank Dan Ingersoll for his continued support and guidance. Funding for this project was provided by the Nuclear Regulatory Commission.

## VII. REFERENCES

1. "BUGLE-80: Coupled 47 Neutron, 20 Gamma-Ray, $P_3$, Cross-Section Library for LWR Shielding Calculations," ORNL RSIC, DLC-075 (1980).

2. C. R. Weisbin, et al, "VITAMIN-E: An ENDF/B-V Multigroup Cross Section Library for LMFBR Core and Shield, LWR Shield, Dosimetry and Fusion Blanket Technology," ORNL-5505(ENDF-274) February, 1979.

3. J. E. White, et al, "Specifications for the Development of BUGLE-93: An ENDF/B-VI Multigroup Cross Section Library for LWR Shielding and Pressure Vessel Dosimetry," ORNL-12230, November, 1992.

4. E. Sartori, "VITAMIN-J, a 175 Group Neutron Cross Section Library Based on JEF-1 for Shielding Benchmark Calculations," JEF/DOC-100 Preliminary, 1985.

5. ORNL, "SCALE: A Modular Code System for Performing Standardized Computer Analyses for Licensing Evaluation," NUREG/CR-200, Rev. 4, Vols. 1, II, and III (draft February 1990).

6. "SAILOR: Coupled, Self-Shielded, 47-Neutron, 20-Gamma-Ray, $P_3$, Cross-Section Library for Light Water Reactors," RSIC DLC-076 (1985).

7. W. W. Engle Jr., "ANISN, A One-Dimensional Discrete Ordinates Transport Code with Anisotropic Scattering," Report K-1693, March, 1967.

8. W. A. Rhoades and R. L. Childs, "The DORT Two-Dimensional Discrete Ordinates Transport Code," *Nucl. Sci. & Eng.* **99**, (1), 88-89 (May 1988).

9. R. H. Johnson, "Integral Tests of Neutron Cross Sections for Iron, Niobium, Beryllium, and Polyethylene," Thesis, University of Illinois 1975.

10. R. E. Maerker, "The ORNL Benchmark Experiment for Neutron Transport Through Iron and Stainless Steel, Part I," ORNL-TM 4222 (1974).

11. R. L. Childs and J. V. Pace III, "GRTUNCL: First Collision Source Program," ORNL (Informal Notes) RSIC Computer Code Collection CCC-484 (1982).

12. Van Baker and R. L. Childs, "FALSTF: Calculator of Response of Detectors External to Shielding Configurations," ORNL (Notes), RSIC CCC-351 (1974).

13. R. E. Maerker, "SDT1: Iron Broomstick Experiment - An Experimental Check of Neutron Total Cross Sections," ORNL-TM-3867 (1972).

14. M. D. Carter, A. K. McCraken, and A. Packwood, "The Winfrith Iron Benchmark Experiment", NEACRP-A-448, March 29, 1982.

15. W. N. McElroy, Ed., "LWR Pressure Vessel Surveillance Dosimetry Improvement Program: PCA Experiments and Blind Test", HEDL-TME 80-87 R5 (also NUREG/CR-1861), July 1991.

16. J. Celnick, "One Dimensional Representation of Light Water Reactor for Prediction of Fluence and Dose Rate Levels at Core Midplane," ESIS Newsletter No. 34 , (July, 1980).

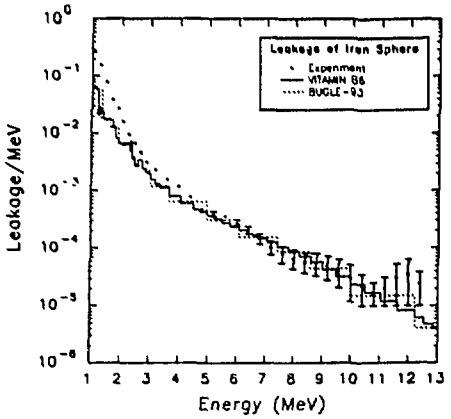


Figure 1. Illinois Iron Sphere Experiment
(Iron Sphere Surrounding a Cf-252 Source)

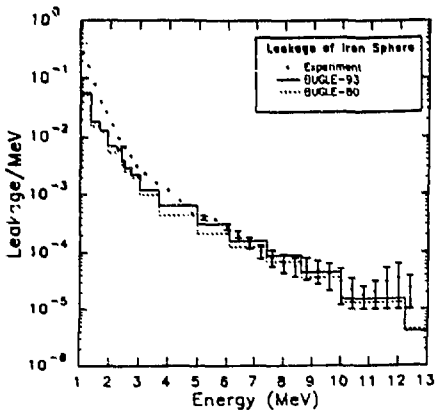


Figure 2. Illinois Iron Sphere Experiment
(Iron Sphere Surrounding a Cf-252 Source)

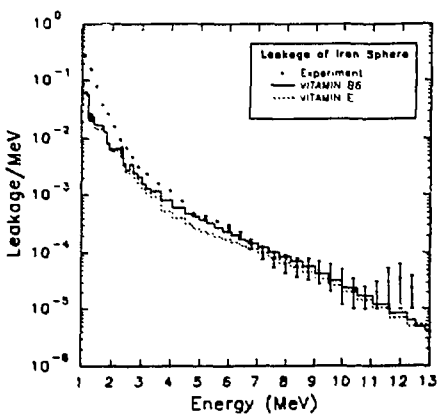


Figure 3. Illinois Iron Sphere Experiment
(Iron Sphere Surrounding a Cf-252 Source)

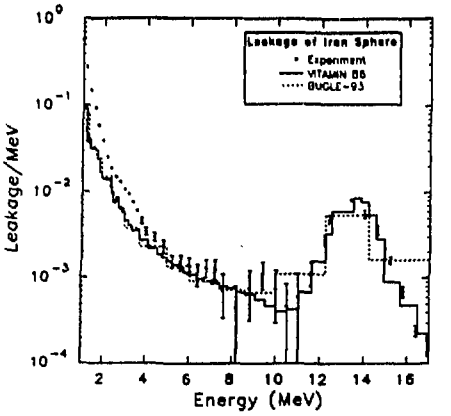


Figure 4. Illinois Iron Sphere Experiment
(Iron Sphere Surrounding a D-T Source)

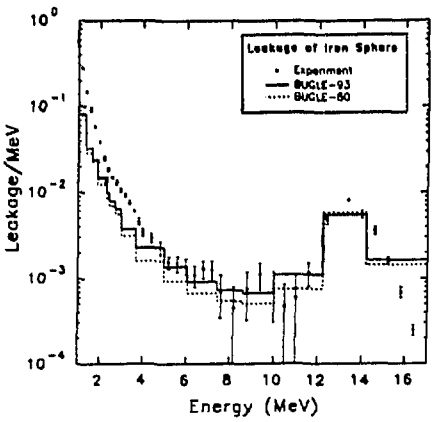


Figure 5. Illinois Iron Sphere Experiment
(Iron Sphere Surrounding a D-T Source)

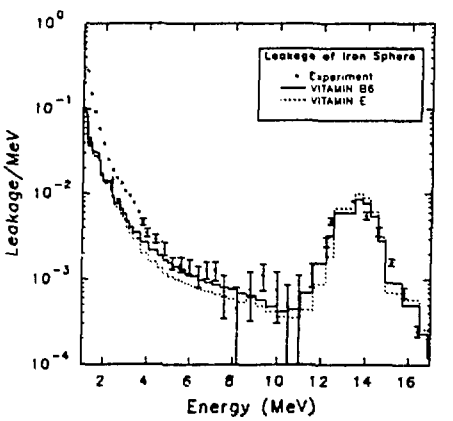


Figure 6. Illinois Iron Sphere Experiment
(Iron Sphere Surrounding a D-T Source)

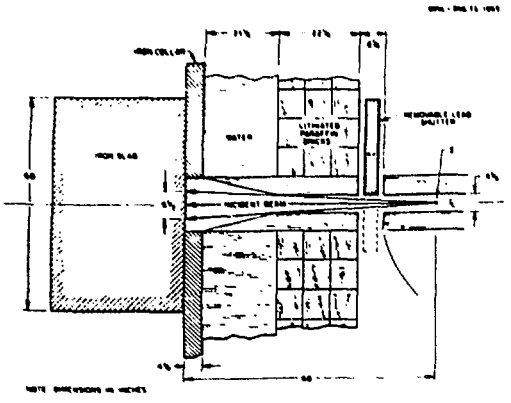

Figure 7. SDT11: Iron Slab Behind Collimated Reactor Neutron Source

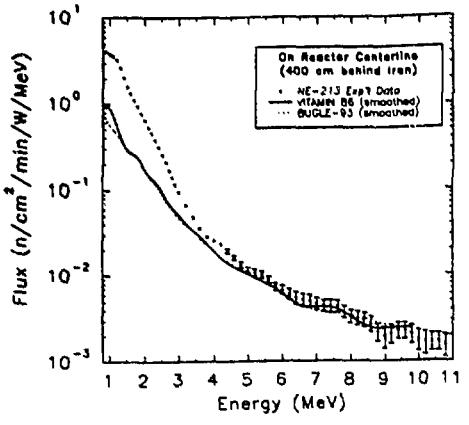


Figure 8. SDT11 Experimental Benchmark Fine & Broad Group Results. (30 cm Iron Behind Collimated TSR)

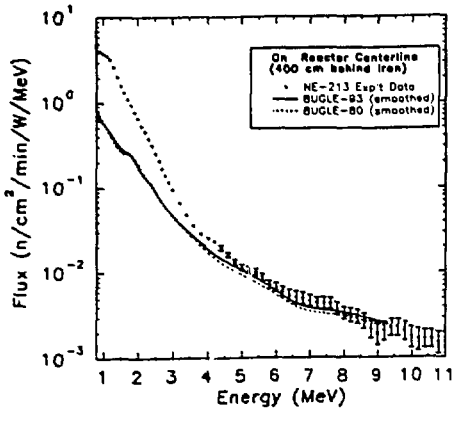


Figure 9. SDT11 Experimental Benchmark Broad Group Results. (30 cm Iron Behind Collimated TSR)

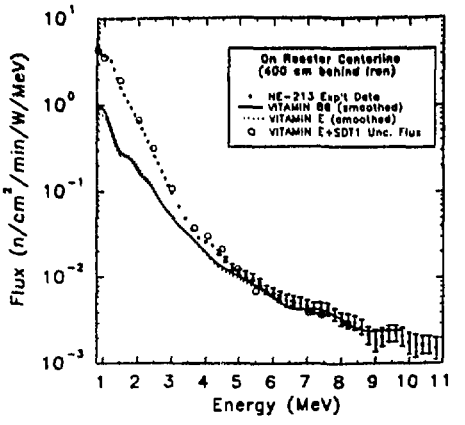


Figure 10. SDT11 Experimental Benchmark Fine Group Results. (30 cm Iron Behind Collimated TSR)

Table 1. SDT11: NE-213 Behind 30 cm of Iron. Ratio of Integrated Calculated to Measured Neutron Fluxes.

| LOCATION | BUGLE-93 | BUGLE-80 | VITAMIN-B6 | VITAMIN-E |
|---|---|---|---|---|
| 15 deg. OC[a] | .819 | .713 | .808 | .728 |

[a]Measurements and Calculation Located Off-Reactor Centerline (OC).

Table 2. SDT11: Benjamin Counter Behind 30 cm of Iron (Fe) and Stainless Steel (SS). Ratio of Integrated Calculated to Measured Neutron Fluxes

| LOCATION | BUGLE-93 | BUGLE-80 | VITAMIN-B6 | VITAMIN-E |
|---|---|---|---|---|
| CL[a] behind Fe | .800 | .795 | .763 | .828 |
| OC[b] behind Fe | 1.00 | 1.00 | .952 | 1.05 |
| CL behind SS | 1.04 | 1.04 | .979 | .938 |
| OC behind SS | 1.09 | .938 | 1.03 | 1.11 |

[a]Measurements and Calculations Located On-Reactor Centerline (CL).
[b]Measurements and Calculations Located Off-Reactor Centerline (OC), 50 degrees

Table 3. SDT11: Bonner Balls (BB) Behind 30 cm of Iron (Fe) and Stainless Steel (SS). Ratio of Calculated to Measured Integral Neutron Fluxes.

| LOCATION | BUGLE-93 | BUGLE-80 | VITAMIN-B6 | VITAMIN-E |
|---|---|---|---|---|
| 3" BB, CL[a], Fe | 655 | .381 | .395 | .469 |
| 3" BB, OC[b], Fe | .853 | .868 | .901 | .913 |
| 6" BB, CL, Fe | 332 | .287 | .318 | .345 |
| 6" BB, OC, Fe | 893 | 921 | .944 | .938 |
| 10" BB, CL, Fe | .231 | .216 | .250 | .251 |
| 10" BB, OC, Fe | .519 | .523 | .540 | .519 |
| 3" BB, CL, SS | .576 | .571 | .623 | .610 |
| 3" BB, OC, SS | .827 | .817 | .877 | .853 |
| 6" BB, CL, SS | .528 | .538 | .571 | .572 |
| 6" BB, OC, SS | .938 | .960 | .978 | .956 |
| 10" BB,CL, SS | .425 | .429 | .453 | .442 |
| 10" BB,OC, SS | .813 | .820 | .828 | .804 |

[a]Measurements and Calculations Located On-Reactor Centerline (CL).
[b]Measurements and Calculations Located Off-Reactor Centerline (OC), 15 degrees.

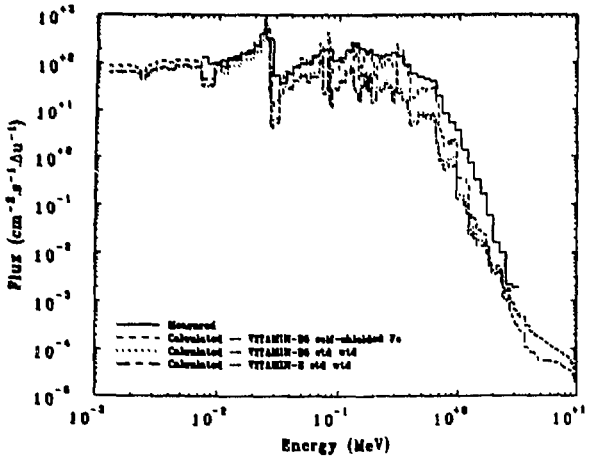


Fig. 11. Comparison of Fine-Group Calculated Neutron Fluxes With Measured Results 76.2 cm Into the Shield of the Winfrith Iron Benchmark.

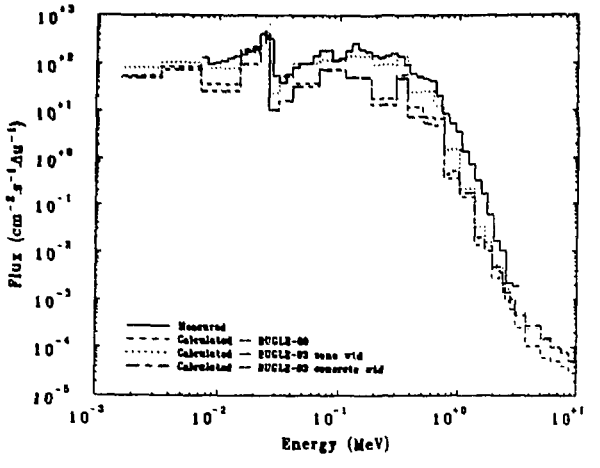


Fig. 12. Comparison of Broad-Group Calculated Neutron Fluxes With Measured Results 76.2 cm Into the Shield of the Winfrith Iron Benchmark.

Table 4. Ratios of Calculated to Measured Integral Neutron Fluxes[a] for the Winfrith Iron Benchmark Experiment.

| Iron Shield Thickness (cm) —› | 20.32 | 50.8 | 76.2 | 101.6 |
|---|---|---|---|---|
| BUGLE-80 | 1.28 | 0.73 | 0.46 | 0.24 |
| BUGLE-93 zone wtd | 1.28 | 0.95 | 0.80 | 0.52 |
| BUGLE-93 concrete wtd | 1.30 | 0.62 | 0.34 | 0.15 |
| VITAMIN-E std wtd | 1.09 | 0.69 | 0.48 | 0.29 |
| VITAMIN-B6 std wtd | 1.12 | 0.65 | 0.42 | 0.21 |
| VITAMIN-B6 self-shielded Fe | 1.28 | 0.98 | 0.87 | 0.62 |

[a]Note: The energy ranges are as follows: 52.5 keV to 4.72 MeV at 20.32 cm, 7.1 keV to 4.72 MeV at 50.8 cm, 7.1 keV to 3.25 MeV at 76.2 cm, and 9.12 keV to 1.97 MeV at 101.6 cm.

Table 5. Ratios of Calculated to Measured $^{32}S(n,p)$ Activities for the Winfrith Iron Benchmark Experiment.

| Iron Shield Thickness (cm) —› | 20.32 | 35.56 | 50.8 | 60.96 |
|---|---|---|---|---|
| BUGLE-80 | 0.88 | 0.80 | 0.60 | 0.51 |
| BUGLE-93 zone wtd | 1.06 | 1.09 | 0.92 | 0.84 |
| BUGLE-93 concrete wtd | 1.06 | 1.06 | 0.89 | 0.79 |
| VITAMIN-E std wtd | 0.87 | 0.79 | 0.60 | 0.51 |
| VITAMIN-B6 std wtd | 1.04 | 1.04 | 0.86 | 0.76 |
| VITAMIN-B6 self-shielded Fe | 1.06 | 1.08 | 0.91 | 0.82 |

Table 6. Ratios of Calculated to Measured $^{103}Rh(n,n')$ Activities for the Winfrith Iron Benchmark Experiment.

| Iron Shield Thickness (cm) —› | 20.32 | 50.8 | 76.2 | 101.6 |
|---|---|---|---|---|
| BUGLE-80 | 1.03 | 0.63 | 0.27 | 0.09 |
| BUGLE-93 zone wtd | 1.18 | 1.09 | 0.73 | 0.39 |
| BUGLE-93 concrete wtd | 1.04 | 0.58 | 0.23 | 0.07 |
| VITAMIN-E std wtd | 0.93 | 0.48 | 0.18 | 0.05 |
| VITAMIN-B6 std wtd | 0.96 | 0.52 | 0.20 | 0.06 |
| VITAMIN-B6 self-shielded Fe | 1.17 | 1.11 | 0.79 | 0.45 |

Table 7. Ratios of Calculated to Measured $^{115}In(n,n')$ Activities for the Winfrith Iron Benchmark Experiment.

| Iron Shield Thickness (cm) —› | 20.32 | 30.48 | 45.72 | 55.88 |
|---|---|---|---|---|
| BUGLE-80 | 0.86 | 0.77 | 0.49 | 0.37 |
| BUGLE-93 zone wtd | 1.00 | 0.99 | 0.75 | 0.65 |
| BUGLE-93 concrete wtd | 0.91 | 0.81 | 0.48 | 0.34 |
| VITAMIN-E std wtd | 0.81 | 0.68 | 0.38 | 0.26 |
| VITAMIN-B6 std wtd | 0.87 | 0.75 | 0.43 | 0.31 |
| VITAMIN-B6 self-shielded Fe | 0.99 | 0.96 | 0.71 | 0.62 |

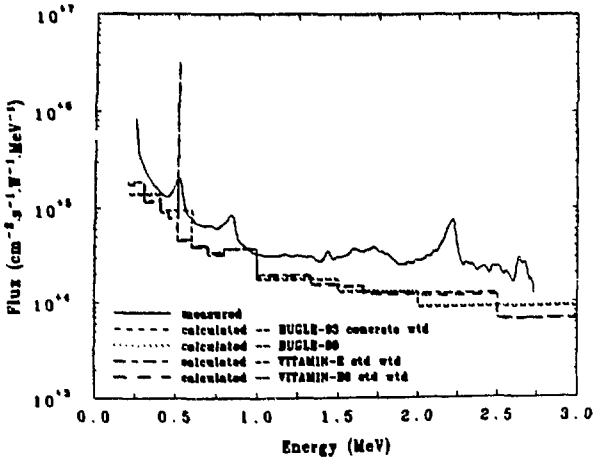


Fig. 13. Comparison of Calculated and Measured 0.248 MeV ≤ E ≤ 2.731 MeV Gamma-Ray Fluxes at the 1/4 T Location of the PCA 4/12 Configuration.

Table 8. Comparison of Calculated and Measured Gamma-Ray Energy Deposition in Steel in PCA Configuration 4/12.

| LOCATION | GAMMA-RAY ENERGY DEPOSITION (mGy·h⁻¹·W⁻¹) | | | | |
|---|---|---|---|---|---|
| | MEASURED | CALCULATED C/E[a] | | | |
| | | BUGLE-80 | BUGLE-93 | VITAMIN-E | VITAMIN-B6 |
| SSC | 33.81 | 33.5<br>1.02 | 33.12<br>1.01 | 33.69<br>1.03 | 33.32<br>1.02 |
| 1/4 T | 2.55 | 2.763<br>1.08 | 2.736<br>1.07 | 2.836<br>1.11 | 2.83<br>1.11 |
| 1/2 T | 0.68 | 0.703<br>1.03 | 0.698<br>1.03 | 0.724<br>1.06 | 0.722<br>1.06 |
| 3/4 T | 0.215 | 0.216<br>1.00 | 0.219<br>1.02 | 0.223<br>1.04 | 0.221<br>1.03 |

[a]Ratio of calculated value to the experimental value.

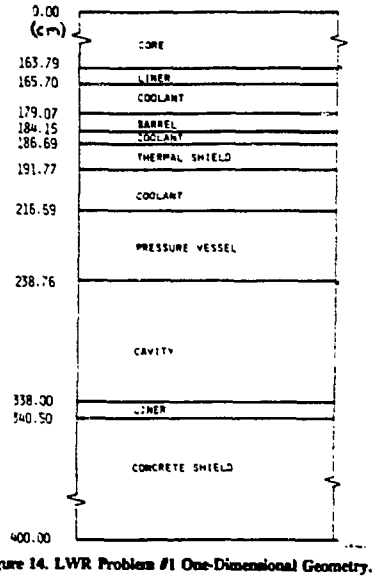


Figure 14. LWR Problem #1 One-Dimensional Geometry.

Table 9. LWR #1 Materials in Zones or Regions.

| Region | Material |
|---|---|
| Core | Homogenized LWR Core |
| Liner | SS-304 |
| Coolant | Water, 580F, 400 PPMB |
| Barrel | SS-304 |
| Coolant | Water, 555F, 400 PPMB |
| Thermal Shield | SS-304 |
| Coolant | Water, 555F, 400 PPMB |
| Pressure Vessel | ASTM-508-CL2 |
| Cavity | Air |
| Shield Liner | A-533-B |
| Concrete Shield | Concrete |

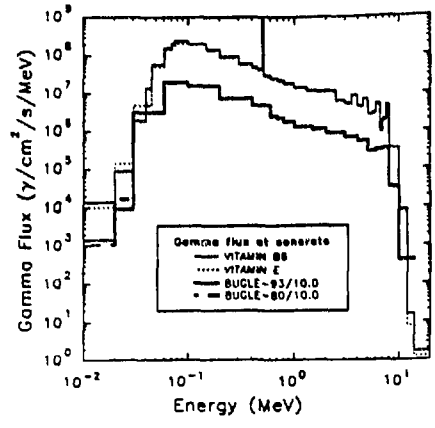


Figure 15. LWR #1 Calculational Benchmark

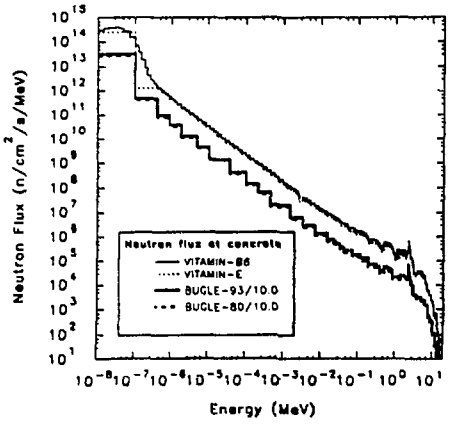


Figure 16. LWR #1 Calculational Benchmark